

Local state space geometry and thermal metastability in complex landscapes: the spin-glass case.

Paolo Sibani

*Fysisk Institut, Odense Universitet
Campusvej 55, DK5230 Odense M
Denmark*

(December 2, 2024)

After a brief review of thermalization phenomena in spin glasses and a more detailed description of a previously introduced method (the lid method) for exhaustive explorations of complex landscapes, we present new data obtained by the lid method. These are the outcome of a large scale numerical effort and lead to a geometrical characterization of the landscape of two and three dimensional spin glasses, in the neighborhood of local minima. The results considerably extend our previous investigation of the same models. We argue that thermal metastability in spin glasses is strongly related to the found near exponential local density of states. We then identify the state space structures which correspond to domains in real space and finally indicate how a hierarchical and droplet picture can be merged into a more comprehensive and consistent mesoscopic description.

75.10Nr, 02.50Ga, 05.40.+j, 02.70.-c

I. INTRODUCTION

The state space of complex systems as spin-glasses, glasses, proteins, molecular clusters and hard combinatorial problems is often described as a ‘landscape’. Technically, a landscape is a graph, where the nodes represent the states of the system, and the edges connect neighbor states. Each node is characterized by a scalar quantity, which in physical system is usually the energy, while in other cases it can be a cost or a fitness function. Often the system dynamics takes the form of a Markov process with states in the landscape. Transitions occur among neighbors, and, in thermal processes, at rates depending on the energy differences and on the temperature in agreement with the requirements of detailed balance. Detail balance ensures that the stationary distribution of the Markov process equals the equilibrium Boltzmann distribution. However, in many cases, including spin glasses, thermalization at low temperatures is very slow and complex, and the system remains far from thermodynamical equilibrium on a very wide range of time scales.

The spin glass case is particularly interesting since the phenomenology of its extended ‘transient’, which at low enough temperatures may well encompass all observable time scales [1,2], has been carefully investigated both numerically [3–6] and experimentally [7–13]. Most experimental spin glass work has been interpreted in the framework of the droplet and domain theories [14–16] or within a hierarchical picture inspired by the ultrametric organization of the pure states of mean field models [17]. Theoretical discussions on the nature of state space [18,19] and of the low temperature relaxation in complex systems [20–23] have continued, offering diverse – if plausible – explanations for phenomena like slow dynamics and aging.

We find that the persistent dichotomy between real space and state space descriptions is unsatisfactory, and that direct numerical investigations are needed to formulate a correct mesoscopic theory which includes both aspects. One crucially simplifying low temperatures feature is that excitations mainly consist of small non-interacting clusters in a frozen environment. This was realized long ago by Dasgupta et al. [24] and recently confirmed in large scale studies of excitation morphology and domain growth [25,26]. Non interacting domains lead to a block structure in state space, where each block contains the accessible states of a single domain. This motivates applying on a larger scale a previously introduced exhaustive enumeration technique [27,28], the ‘lid’ method, which addresses rather directly the issue of landscape structure of small lattices. In this paper we describe new data on state space geometry obtained by the lid method, and combine them with our previous investigations of domain growth. Our conclusion is that a certain type of hierarchical structure can be associated with the highly constrained configuration space of a growing domain.

In the sequel, we first present as a background relevant low temperature dynamical features of spin glasses. We then describe the lid method and the results obtained by it regarding models with nearest neighbor Gaussian distributed interactions. Finally, we consider the evidence on the low temperatures dynamics and state-space structure of spin-glasses and discuss relevant phenomenological models.

The extensive calculations required in this investigation were done on a Silicon Graphics Onyx parallel machine with 24 processors and 2 gigabytes of RAM at the University of Odense, Denmark, and on a Silicon Graphics 32 CPU

Origin2000 with 8GB of memory kindly made available to this project by the SGI Advanced Technology Centre in Cortaillod, Switzerland.

A. Background

Stochastic dynamics of short range spin glass models with Gaussian distributed interactions closely mimics the relaxational properties of real samples [3]. One can therefore conveniently combine detailed information from numerical simulations of these models with experimental insights. Valuable dynamical information on spin glasses obtained through numerical and experimental aging studies is usually interpreted in terms of properties of the free energy landscape. Yet, considerable disagreement remains on what these properties might be, perhaps unsurprisingly, given the indirect nature of the evidence.

The defining characteristic of aging behavior is the discovery [7,8] that the linear response to a change in an external field strongly depends on the waiting time t_w spent by the system at low temperature *previous* to the change. In a Zero Field Cooled (ZFC) experiment [11], the system is rapidly cooled in zero field to a temperature T_m and is then left undisturbed a time t_w . Thereafter, a small magnetic field is turned on, and the growing magnetic response of the system is measured. In a Thermo Remanent Magnetization (TRM) experiment [12] the system is quickly cooled to T_m and then allowed to relax in a magnetic field for a time t_w . The field is then cut and the decay of the magnetization is measured.

A generally used method of exploring free energy barriers is to repeat two or more times an entire experimental protocol, each time with different waiting times and temperatures. The first experiment provides a reference curve. In a second experiment, waiting times and temperatures are changed together in such a way that the same experimental curve is produced. The interpretation is that the same region of state space is explored, in one case within time t_w at temperature T_m and in the other case within time t'_w at temperature T'_m . Numerically, domain growth was studied [26] by a protocol very similar to the one just described. We found that temperature changes could be fully compensated by changes in the simulation length, (a smooth rescaling of time) as long as the temperature remained below a well defined threshold, at which - arguably - the structure of the free energy landscape changed dramatically. More complicated experiments have also been performed, which feature small changes of temperature and external field during the aging time. The effect of these procedures is to partially or completely *reset* the system age, in the sense that the location of the inflection point moves away from the true value of the waiting time. Broadly speaking, the experimental results show that the free energy landscape must possess geometrical features which make memory behavior possible. These features must be captured by mesoscopic models [23] but should also be checked directly at a microscopic level.

The free energy landscape is a mesoscopic concept which applies to systems with multiple metastable states and where relaxation happens under conditions of *local equilibrium* (or *partial thermalization*). A useful heuristic picture of relaxation in complex landscapes which explains and builds upon the concept of partial thermalization is known as ‘broken ergodicity’ [29,30]. This term should be contrasted to ‘broken symmetry’ which characterizes systems like ferromagnets and where the magnetization is an easily identified order parameter: there, below the critical temperature, state space breaks up in two non-communicating ‘valleys’, with positive and negative magnetizations respectively, one of which is selected for equilibration. By contrast, in broken ergodicity there are many valleys, rather than just two. Each is a subsets of state space in which relaxational dynamics lingers for sufficiently long time for the system to approximately thermalize. Therefore, on certain time scale the system will appear non ergodic. Whether or not this is actually true in the thermodynamic limit and for infinite times is unimportant here, as we only deal with issues of metastability. It is then sufficient that ergodicity be broken on relevant experimental time scales.

When local thermal equilibrium prevails, the probability distribution (obtainable in principle by solving a master equation) is close to a Boltzmann distribution within each valley, except for slowly changing time dependent multiplicative factors reflecting the flux of probability from one valley to the other [23]. Within a certain experimental time window, measurable quantities will then be canonical averages over the microstates belonging to the valley. Therefore, it is physically reasonable to lump all these states into one point of a *free* energy landscape. A local – and slowly time dependent – partition function $Z_\alpha(T)$ can be defined in the usual way, but with the summation index restricted to states belonging to valley α . The free energy of the valley is then defined by the relation $F_\alpha = -T \ln Z_\alpha$. In the above formulae T is the temperature, and the Boltzmann constant has been set to one. It is worth keeping in mind that in high dimensional spaces regions surrounding a saddle point with one (or just few) unstable direction will also be metastable [21], and thus qualify as valleys in our terminology. The slow dynamics in the free energy landscape generally depends on the connections and on the free energy differences between valleys.

Three mechanism seem important in determining the course of thermal equilibration and thus the shape of the free energy landscape: energy barriers, entropic barriers or bottlenecks, and the effect of the local density of states.

The energy barrier between any two microscopic states a and b is defined by a min-max procedure. First the highest energy along each path joining a and b is calculated. Then the barrier is obtained as the minimum of this quantity over all possible paths.

An entropic barrier is a more subtle concept and much harder to quantify: at low enough temperature and within a certain fixed time scale, high energy configurations are dynamically forbidden. The remaining part of the landscape may then acquire a convoluted topology, in which different states possess a greatly varying number of accessible neighbors: Subregions can exist which are internally highly connected, but sparsely connected to each other. This difference in effective connectivity - a dynamical bottleneck - can give rise to partial equilibration even without conspicuous energy barriers *along* the paths leading from one subset to the other.

The third mechanism, which we strongly emphasize, is the effect on equilibration of the local density of states within a valley. In general, the quasi-equilibrium probability to find the system in a state of energy E contains the product of a Boltzmann factor with the number of states at that energy which are ‘locally’ available to the dynamics on relevant time scales. Only if the local equilibrium distribution strongly favors low-energy states will the flux of probability over the saddles from one valley to another be small, and only then is it meaningful to treat different valleys as weakly coupled. If the local density of states is strongly increasing with energy, the Boltzmann distribution can become ‘top heavy’ and metastability can be lost.

Dynamical processes following rapid changes of external parameters which disturb the quasi equilibrium relaxation, (e.g. like the age reset following field or temperature changes) can involve properties of the system beyond those of its free energy landscape [23,31].

B. The lid method

The lid method is an exhaustive enumeration of (relevant) parts of the energy landscape of the system. Inferences regarding the free energy landscape have therefore to be indirect. In particular, while we can explore in detail the first and third of the confining mechanisms just described, we cannot directly address the question of entropic barriers since an exhaustive method is by its nature insensitive to bottlenecks.

As the number of configurations which must be accounted for grows exponentially with the size of the system, only relatively small systems can be analyzed. In two dimensions up to linear size 10, and in three dimensions up to linear size 6. Although these sizes may seem small, they compare very well with typical domain sizes in low temperature relaxation [25,26] as well as with the lattice sizes used in much of the early work on the critical properties of spin glasses [32–35].

In the following we only give a qualitative account of how the lid method works. A more technical description of the algorithm, including its parallel implementation and performance statistics, is planned for a separate publication [36].

Consider the set $\mathcal{P}_{\psi,L}$ of all states which can be visited, starting from a local energy minimum or reference state ψ , without ever exceeding an energy barrier L . In a thermal relaxation process, the ‘typical’ time needed to exit $\mathcal{P}_{\psi,L}$ (whether it be a first passage time or an average) will contain a factor $\exp(L/T)$, which grows large at low temperatures. Therefore, \mathcal{P} is a bona fide candidate for a metastable region operationally defined by an energy barrier. Following our previous notation [27] we call \mathcal{P} a pocket of depth L centered at state ψ , rather than a valley, in order to emphasize that a pocket is not necessarily metastable at all temperatures. *All* states in the pocket are generated by an exhaustive search algorithm, and various geometrical properties are then calculated.

To visualize how the lid method works, imagine pouring water into the landscape, thereby forming a lake covering a local minimum ψ . Initially, ψ will be the deepest point of the lake, but eventually, another point of lesser height ψ' might become submerged. If this happens a watershed is crossed and the valley belonging to ψ' is flooded. Loosely speaking, the term ‘deep’ local minimum is used to indicate a local minimum such that a new basin is not discovered ‘too soon’ in this gedanken flooding process. Clearly, the ground state should qualify as a deep minimum, but a more specific context is needed for an operational meaning. A natural way seems to be a distance criterion: a minimum is ‘deep’ if the distance from the rim of the lake to the location of deepest submerged point is sufficiently large. In spin-glasses a suitable distance is the Hamming distance, which is the least number of spin flips needed to move from one configuration to another. More generally, the least number of edges which must be traversed to go from one node of a graph to another is a measure of distance which can serve our purpose.

We now consider a deep minimum and define for concreteness the origin of the energy scale by setting its energy to zero. The amount of landscape submerged as a function of the depth of water poured provides a first simple measure of the shape of the pocket, which we call its volume, $\mathcal{V}_{\mathcal{P}}$. One can further ask about the height distribution of the submerged points - which is the local density of states $\mathcal{D}_{\mathcal{P}}(E)$. Depending on the problem at hand, additional questions can be asked: what is the height of the lowest saddle which must be reached before the water can flow to

the ‘sea’ - i.e. - before the flooded part of state space percolates. And how does this height scale with some important parameter of the problem - e.g. its size (number of atoms or spins) - or the value of an external field. These properties are all local as they do not depend on properties of the landscape outside the pocket itself. In the spin-glass case, the percolation threshold is reached when the energy is sufficiently high to allow the reversal of the reference state.

The lid algorithm can deal with pockets of any depth, not just deep ones. One can pick a reference state randomly, and terminate the exploration when a lower energy state is found. By iterating the procedure from this new state, one can turn the lid algorithm into an extremely fast, albeit very memory intensive, optimization tool.

II. RESULTS

We consider a set of \mathcal{N} Ising spins $\sigma_i = \pm 1$ placed on a 2D or 3D cubic lattice with periodic boundary conditions. The energy of the x ’th configuration, $0 < x \leq 2^{\mathcal{N}}$, is defined by the well known Hamiltonian [37]

$$E(x) = -\frac{1}{2} \sum_{i,j} J_{ij} \sigma_i(x) \sigma_j(x), \quad (2.1)$$

where $J_{ij} = J_{ji}$ and where $J_{ij} \neq 0$ only if spins i and j are adjacent on the grid. In this case, and for $i < j$, we take the J_{ij} ’s as independent gaussian variables, with zero average and variance $J^2 = 1$. This last choice fixes the (dimensionless) energy and temperature scales. Neighbors configurations are by definition those which differ in the orientation of exactly one spin.

In each dimension we studied lattices of different linear sizes. For each size we generated 25 realizations of the J_{ij} ’s, and again for each of these we found one or more very low energy configurations or reference states. Starting from each reference state we calculate 1) the available volume $\mathcal{V}(L)$ for $L \leq L_{max}$, 2) the distribution in energy of the states, i.e. the local density of states $\mathcal{D}(E, L_{max})$. 3) The distribution of Hamming distances relative to the reference state and in particular the average and maximal Hamming distance achievable for a given barrier. 4) The average number of neighbors to which a state is connected, as a function of the lid. This number would be constant and equal to the number of spins if all neighbors were available, but as high lying states are discarded, the effective connectivity is much lower, illustrating our point about entropic barriers.

In most cases L_{max} is chosen equal to the least barrier L_{rev} , which allows the systems dynamics to access the spin reversed state $-\psi$. L_{rev} depends in general on the system size and is defined as the least energy for which half of the spins in the reference configuration can be flipped. By symmetry, it is possible from a state of energy L_{rev} to flip the rest of the spins at no further energy cost. Unfortunately, for the 6^3 system it was not possible to do an exhaustive enumeration up to L_{rev} . The searches stopped at various energies when a memory limit (7.8 gigabytes) was reached.

If, while attempting an enumeration up to L_{max} , a state with lower energy than ψ is discovered, the calculation is discontinued and started afresh from this state, which thus becomes the new reference. This procedure operationally defines a deep minimum configuration as one which can be reverted without encountering a lower energy state. In practice, one starts with a randomly chosen ψ , and lets the algorithm successively discover deeper and deeper minima, until one is found which either fulfills the reversal criterion or which could not be further improved during the exhaustive search.

As customary in numerical investigation of disordered systems, averages are performed over many different realizations of the couplings. However, we also try to convey an idea of the system to system and pocket to pocket variation.

Our data are rather simply parametrized: the local density of states is almost exponential, with a systematic downward curvature. In a semilogarithmic plot the curvature is fully accounted for by a parabola, which has a very small second order term in the 3D case and a somewhat larger one in 2D. The available volume in the pocket is also close to an exponential function of the lid energy, if one smooths out the jumps which occur when a new ‘side pocket’ is accessed as the barrier increases.

One could imagine that most of the states in the pocket would have energies close to zero, with just a few extra states acting as connections among subvalleys. If this were the case, the local density of state would be strongly peaked at zero, while in fact it closely follows the volume vs. lid curve. This shows that the great majority of the states which become accessible by a small increment of the lid has energies right below it.

A. 2D system

There is widespread agreement [32,38,39] that the 2D dimensional Ising spin-glass model with Gaussian distribution of bonds has a $T = 0$ transition temperature. Nevertheless, 2D systems certainly possess metastability and a complex

low temperature relaxation patterns similar to those characterizing their 3D counterparts, including slow relaxation and aging [10].

We were able to study systems of linear size 4, 5, 6, 7, 8, 9 and 10. For each size we considered 25 ‘deep energy minima’ belonging to different realizations of the couplings. For each of these, an exhaustive enumeration was performed terminating at the reversal barrier L_{rev} in all but one of the 10^2 cases. In this last case where we were able to flip 48 spins rather than 50, before abandoning the calculation due to lack of computer memory.

As the barrier allowing access to the reversed state varied from sample to sample, the corresponding pockets also greatly fluctuated in size. For easiness of display, the total volume of each pocket was used to normalize the corresponding density of states, resulting in parallel shifts in the semilog plots.

In all cases we have a close to exponential dependence on the energy, spanning, in the 10^2 case several decades of data, as shown in Figure 1. The raw data are indicated by plusses, while the full lines are calculated by fitting $\log(\mathcal{D}(E, L_{max}))$ to a second order polynomial in E . The coefficient of the second order term is typically 20 times smaller than the coefficient of the linear term. For reasons explained later, the reciprocal of the linear coefficient is a putative ‘kinetic transition temperature’ T_k .

The data shown all stem from the the 10^2 systems, with the different curves pertaining to different realization of the couplings. The corresponding data for the other system sizes have a similar outlook. However, the quality of the fits is lesser for smaller sizes, as one would expect.

In Fig.2 we plot the calculated 25 values of T_k as a function of the linear size of the system. As one would expect, as the size increases the spread in the data decreases. The average values, which is indicated by a circle, also decreases with system size.

The data shown in Fig.3 describe systems ranging in size from 4^2 to 10^2 . In each case we display the largest Hamming distance found in the pocket delimited by a given energy barrier as a function of this barrier, which is additionally averaged over 25 realizations of the disorder. The Hamming distance is scaled down to the unit interval to ease comparisons among the different sizes. Thus, reversal of the reference configuration is achieved for the value .5 of the ordinate, and corresponding values on the abscissa are the average reversal barriers. The curve which is highest in most of its range belongs to the smallest system, while the lowest curve belongs to the largest system. Note how the the average exit barrier increases with system size, but does so at a decreasing rate. This is to be contrasted to the 3D behavior, where the exit barriers strongly increase with the linear size.

B. 3D system

The analysis for the 3D case mainly follows the same outline as in 2D. The three dimensional problem is computationally far more demanding, partly because the number of spins grows faster with the linear system size, but also because the exit barrier grows strongly with the size. For these reasons, were only able to complete the enumeration up to L_{rev} for linear sizes 3, 4 and (in 23 out of 25 realization of the disorder) 5. The analysis of systems of linear size 6 were done on a computer with 8 gigabytes of RAM. Yet we could not reach the reversal barrier, and we set the program to stop the search when 81 spins had been flipped or 7.8 gigabytes of RAM were allocated, whichever happened first. In practice we ended up counting between 50 and 80 millions of configurations before being forced to stop.

In 3D we additionally performed two different types of investigation, which are presented right below: 1) for one particular realization of the 5^3 systems, we varied the initial conditions of the search leading to the reference state and 2) for one particular realization of a 6^3 system we studied the local density of states for ‘shallow’ rather than deep minima.

As a few percent of the states are energy minima [27,28] it is to be expected that different *quenches* lead to different end states. In our case, however, the reference states were not produced by quenches, but by careful optimization. Yet we found different reference states, with *disjoint* pockets. The fact that the pockets are indeed different is demonstrated in Fig. 4, where we plot their volume \mathcal{V} vs. L . To avoid partly overlapping data points we multiplied the data by different factors, as indicated in the figure itself.

In the second investigation we consider a sequence of five shallow pockets. The data for pocket #1 are generated by starting the search algorithm at a high lying minimum, and stopping the exhaustive search as soon as a lower minimum is found. This newly found minimum then serves as a starting point for the search leading to the construction of pocket #2, and so on. The whole process describes pockets successively encountered by the search algorithm as it digs its way down into the low energy part of the landscape. Figure 5 shows the local density of state found in each of those pockets. It is interesting that the local density of states as well as of the volume (not shown) are still close to exponential functions of their arguments. Indeed, this behavior generically appears in all the pockets we examined, regardless of the energy of the reference state.

Figure 6 shows the density of states obtained for 25 different 5^3 systems (the same normalization procedure as in the 2D case was used). Again, the raw data are indicated by plusses and the full lines are fits of the logarithm of \mathcal{D} to a parabola. The second order term obtained in the fit is of the order of 1/50 of the linear term.

In Fig. 7, the putative kinetic transition temperature T_k obtained as the reciprocal of the coefficient to the linear term in the expansion of $\log \mathcal{D}$ vs. E are plotted as dots for each linear size and for each of the instances considered. Furthermore, the disorder average of T_k is indicated by a circle for each size. We see that as the size grows, the distribution of T_k gradually sharpens and moves to lower values, past the value for the transition temperature, which is around 0.85 [38,40].

In each of the curves displayed in Fig. 8, the ordinate is the highest Hamming distance which can be achieved for a given barrier and the abscissa is the energy barrier averaged over the disorder. From top to bottom the curves describe systems of linear sizes 3 to 6. The disorder averaging is performed over 25 realizations for the two smallest systems. In the 5^3 case the exhaustive enumerations had to stop short of L_{rev} for three realization of the couplings. In the 6^3 case we were only able to flip 81 spins in about ten instances, while in the other cases the number flipped varied from 41 to 80. In order to avoid introducing a bias in the calculated average curve - we only used the data which were available for all systems.

III. DISCUSSION

In this section we discuss some of the phenomenological approaches found in the literature in relation to our present results. We start elaborating on the physical picture of metastability which our data support, also considering evidence from previous investigations on the excitation morphology of spin glasses [25,26]. Secondly, we argue that domain and hierarchical pictures can be merged in a consistent manner, and that trees are very good mesoscopic models of the low energy parts of spin glass state space. We then more specifically compare with available theoretical descriptions of spin-glasses. We conclude arguing that other complex landscapes might share the the geometrical features found in spin glasses. Some of the arguments in the first part of the discussion can be found in Refs. [25–28] and are included here for the sake of completeness.

A. Exponential local density of states, metastability and slow growth

Investigations of the excitation morphology in large spin-glass systems is nicely complementary to configuration space analysis. Consider the size distribution of clusters of spins which can be overturned from a low energy state by overcoming a certain energy barrier [25] or thermally excited in a time t at temperature T [26]. At low temperatures these clusters remain small, and grow algebraically in time, with temperature dependent exponents. Equivalently, their growth is exponential as a function of a (t, T) dependent variable, which is basically (but not quite) the Arrhenius barrier $b(t, T) \approx T \ln(t)$. Above a well defined temperature - which in 3D closely matches the actual critical temperature - the growth changes qualitatively and becomes very fast. Similar conclusion apply to the way in which domain forms after a quench from a high energy state. This process was simulated in Ref. [26] by applying an algorithm originally suggested by Huse [41]. We emphasize two aspects from the above studies: 1) All low energy excitations consist of clusters of few dynamically active spins in frozen environment. Therefore, studying the state space geometry of small systems provides information which is relevant for large systems as well. 2) The qualitative change of behavior in the growth curves, is indicative of a kinetic transition. This issue is not simply related to the existence of a true equilibrium transition or lack thereof, as indicated by the fact that the dynamical change appears already at short times and independently of dimensionality.

It is easy to see how an exponential density of states generates a kinetic transition by a loss of metastability. The mechanism was rigorously described – within a tree model – by Grossmann et al. [42] and Hoffmann et al. [43]. A qualitative explanation is as follows: as previously, let T_k be the scale parameter characterizing the exponential growth of the density of states within the trap. If the trap is metastable than it must be possible to establish local thermal equilibrium on some time scales. This means that the quasi-equilibrium probability distribution $P(E) \propto \exp(-E/T + E/T_k)$ must be strongly biased towards low energy values. Obviously, this is only possible if $T < T_k$. The trap ceases to be a thermal attractor when the temperature exceeds T_k . This scenario does not change qualitatively if the logarithm of the density of states has a small negative quadratic correction, as seen in our data.

Identifying the small systems studied here with the isolated clusters of similar size which are dynamically active in a large system yields a qualitative explanation of the loss of metastability in spin glasses. The identification can admittedly only be approximately correct, since: 1) the interaction of the clusters with their environment is not the

same as in our present investigation, where we use periodic boundary conditions. 2) as we neglect entropic barriers, we might overestimate the number of states dynamically available to relaxation.

The range of T_k in Figures 2 and 7 includes the values found in Ref. [26]. Consider for example our 4^3 systems: By our identification clusters of corresponding size embedded in a large system would loose their thermal metastability at or above $T = 0.8$. This would create a lot of loose spins, which could arguably trigger a change of kinetic behavior and even a phase-transition. In this situation it may not matter that the 6^3 clusters in isolation would be stable down to a lower temperature. Even though we presently lack an understanding of how the clusters interact we do think that the fact that they melt due to their exponentially growing density of states plays an important (but not exclusive) role for thermal metastability of large systems.

In Monte Carlo simulations [26], the average size of a domain in real space, V_{rs} , grows algebraically in time. The growth exponent is itself an increasing function of the temperature. In configuration space we can consider the number of states V_{cs} visited n t steps by a Monte Carlo algorithm at temperature T . We already have unpublished evidence that V_{cs} grows algebraically. However, we can also conclude that this must be the case from the present evidence. This requires the additional assumption that, starting from zero energy, states of energy b are reached on a time scale $\alpha(T) \ln t$. An Arrhenius behavior corresponds to $\alpha(T) \propto T$. We more generally expect $\alpha(T)$ to be a growing function of T . Since, as we have shown, the volume of the configuration space ‘below’ b increases exponentially with b , we find $V_{cs}(t) \approx t^{C\alpha(T)}$, where C is some constant. Identifying the configuration space as belonging to the spins in a cluster means that $V_{cs} \propto V_{rs}^\beta$ for some constant β . Since, for independent spins, we would have an exponential relation $V_{cs} = 2^{V_{rs}}$, this much slower dependence implies that spins within a cluster are strongly constrained in their dynamics. In other words, relaxation is predominantly sequential [44], which is again consistent with the fact that most configurations are energetically unavailable. Even though the sequential mode of growth characterizes each cluster, there is a parallel relaxation mode as well for the system as a whole: Clusters have a statistical distribution of sizes, and being spatially separated they mainly grow independently of one other.

B. Spin glass phenomenologies

Theoretical descriptions of spin glasses either use insights and numerical observations on the morphology of excitations at low temperature [14–16,24] or build on ideas about the structure of state-space [12,45–51]. The first type of approach is rooted in a renormalization group approach developed by Mc Millan [32] and Bray and Moore [33]. It includes domain or droplet theories [14–16], which emphasize correlation functions and their temperature and field dependence. The early work of Dasgupta et al. [24] is mainly numerical, but also contains interesting theoretical observations on the excitation morphology, which subsequently have been largely ignored. Other approaches are either inspired [12] by the Parisi equilibrium solution of the Edward-Anderson mean field model [17,37] or use a dynamically motivated lumping procedure to produce hierarchical models of state-space, within the general approach of broken ergodicity [46–48]. Campbell’s approach [45] is to describe the spin-glass transition as a percolation transition in state space.

It has been proposed [13] that in order to discriminate between hierarchical and droplet models one should consider their predictions regarding the effect of small variations of temperature and/or magnetic field during the waiting time. Such variations produce very interesting reinitialization effects whose interpretation remains however controversial. In the basic ZFC aging experiment, the logarithmic derivative of the ZFC magnetization, also called relaxation rate, $S(t) = dM(t, t_w)/d \log t$ has, as a function of t , a distinct maximum at $t = t_w$. When, during the waiting time and immediately before the application of the field, the temperature is changed by a pulse of short variation and small amplitude, – up and down or down and up from the measurement temperature T_{m-} , one sees [3] that the maximum of $S(t)$ changes from the actual waiting time to one at very short time. For intermediate values of the pulse amplitude two maxima coexist. The same effect has been observed in Monte Carlo studies [5] where (positive) temperature cycling as well as field and bond cycling were applied. The description of these experiments in terms of an overlap length is fairly straightforward: two maxima indicate the coexistence two lengths, characterizing the old and new domains respectively. In Ref. [4] the reinitialization effect is demonstrated for the out of phase component of the ac susceptibility, which is measured continuously after the quench, while the temperature is subject to both positive and negative temperature pulses. The same set up is used in the experiment of Lefloch et al. [13]. The temperature cycling after the quench consists of a period t_1 at temperature T_m , followed by another period t_2 at a slightly lower respectively higher temperature, after which one returns T_m . The point of Lefloch et al. is that the negative temperature cycling has no effect on the measurement, as cutting away the data taken during t_2 and pasting the remaining two parts of the curve together yields data indistinguishable from those obtained without temperature cycling. This is however not the case with the data of Andersson et al. The asymmetry between negative and positive temperature cyclings is interpreted in Ref. [13] as evidence for a hierarchical free energy landscape closely resembling

that of long range spin glasses, but with metastable states replacing the pure states. On the other hand, Andersson et al. claim that no concept like the overlap length exist in hierarchical models.

We think that the dichotomy between real space and configuration space descriptions is moot. A useful synthesis can be obtained by assigning metastable regions of state space to real space domains. Domain growth then matches the growth of the state space volume which is available to relaxation within a certain time scale. The identification is only possible if domains are small and non-interacting patches of thermally active spins surrounded by a frozen environment, and correspondingly, state space is shattered into separated regions. In either approach one can qualitatively explain the basic aging behavior, and in particular the cross-over between quasi-equilibrium and non-equilibrium dynamics at $t = t_w$.

Our point of view concurs with the earlier cited investigations of Dasgupta et al. [24] and agrees with ideas of Campbell [45] on the structure of available state space at low temperatures. The fact that thermal excitations on small length scales are important precursors of a phase transition is at variance with conventional wisdom, according to which critical behavior is solely determined by long wavelength thermal excitations, and hence depends on the dimensionality of the lattice, but not on the details of the interactions. The fact that spin glass critical exponents are indeed non-universal was demonstrated in a recent numerical study by Bernardi and Campbell [40].

Another point of academic contention [18,19] is the nature of ground states. Apart from obviously degenerate models as the $\pm J$ model, it seems hard to establish by numerical means whether spin-glasses have or do not have a unique ground state, modulo an over-all spin flip. However, Fig. 4 shows that even rather small systems have multiple ‘deep minima’ (for the same realization of couplings), with non intersecting pockets. To be more specific, let ψ_1, ψ_2 be two different reference configurations. For each of them – for instance ψ_1 – it is possible to reach the reversed state $-\psi_1$ by overcoming a barrier $L_{rev,1}$ without visiting *any* state belonging to the other pocket. The question of whether the saddle leading from ψ_1 to $-\psi_1$ also gives access to ψ_2 is not settled by our present calculation, because the enumeration stops (in order to limit memory usage) as soon as the reversal barrier is reached. The fact that we have multiple states which are unrelated by symmetry and which have very low and slightly different energies, seems rather close to having multiple ground states.

It seems reasonable that field or temperature fluctuation which destroy local equilibrium and change the barrier structure could induce transitions from one pocket to a different one. In real space this implies a partial obliteration of the pre-existing thermalized domain structure, which relates well to the chaotic sensitivity of thermal correlations to temperature and field changes [14]. If this interpretation is correct, the breaking of domains which follows temperature or field cycling is simply not a property of the free energy landscape.

Let us finally turn to the relevance of hierarchical models, a variety of which exists in the literature. Consider a tree obtained by successive branchings from a ‘top’ or root node. When endowed with a stochastic dynamics, it already provides a mathematical model of complex relaxation. The structure can be viewed as 1) a hierarchy of energy or free energy barriers, with all the states lying at the bottom of the tree [52,53], or 2) all nodes in the tree may represent (lumped) physical states [42,43,47,54,55]. In the first case, but not in the second, the system has an ultrametric distance, which, for any two bottom nodes is the number of levels up to the root of the smallest subtree which includes them both. Ultrametricity imposes restrictions on the state space geometry well beyond those of a tree structure. A further restriction is imposed if one wishes to identify the index of the hierarchy with a magnetic overlap.

Our numerical results indicate that tree structures where the weight attached to the nodes is exponentially increasing with the level (and the energy), offer a basically correct lumped picture of the state space of a growing domain. The agreement concerns the exponential relation between the volume of a pocket and the size of the barrier which confines it, and the form of the local density of states. These growth laws characterize not only the deep pockets which we have studied extensively, but also the numerous ‘side-pockets’ which merge into them, as shown in Figure 6. The fact that side pockets have different depths is captured by the LS tree of ref. [55], which has non-degenerate energy minima. We finally note that, in the hierarchical models described in Refs. [46,48–51,31] the thermally averaged Hamming distance of states of the model to the initial configuration grows as a power law of time. With the identification we presently propose, this Hamming distance is just domain size, which, as mentioned, displays the same type of algebraic growth.

Explicit numerical evidence pointing to the hierarchical nature of state-space relaxation is provided by the relaxation trees calculated (for small systems) in Refs. [27,28] by explicitly carrying out the coarse graining implied in broken ergodicity. At successive times, all configurations in quasi-equilibrium with one another were identified and lumped together. This procedure yields a tree, where the ‘vertical’ direction is time (or rather its logarithm) and where points represent equilibrated subset of state space, which successively merge with one another.

Admittedly tree models make use of drastic simplifying assumptions on the connectivity which cannot be taken ad literam; still they respect the basic geometrical features of the landscape. As in addition thermal induced hopping on tree structures reproduce the known spin-glass phenomenology, including reset phenomena [46–51,31], these models provide a physically sound lumped picture of spin-glass landscapes.

IV. CONCLUSIONS

The combined evidence from exhaustive explorations of state space regions which surround deep local minima and from Monte Carlo investigation of domain growth supports the following conclusions on the geometry of the spin-glass state space at very low energies:

- 1) Small length scale excitations are quite important for the low-temperature relaxation behavior. Their state-space counterparts are isolated pockets of states which surround deep energy minima, and which are characterized by: a) low internal connectivity, b) near exponential increase of the available volume as a function of the highest energy barrier crossed, and c) near exponential density of states. These features produce a thermal instability, which is a precursor of a phase-transition, when such occurs, as indicated by the fact that the kinetic transition temperature associated with the exponential density of states is close to the true transition temperature of the systems.
- 2) There are many deep energy minima or reference states, which are unrelated by symmetry operations and which are surrounded by disjoint pockets i.e., the energy barrier leading from one pocket to the other is at least as high as the barrier which permits the complete reversal of the reference state. Partial destruction of thermal correlations following changes in external parameters corresponds to (part of) the system jumping from one pocket to another - not related to the first by a symmetry operation. 3) Relaxation within the pockets is itself a slow process, due to internal energy and entropy barriers. This slow relaxation appears in real space as the algebraic growth of domains and in state space as slow algebraic diffusion. The domain and state-space descriptions can thus be unified.

It is interesting to speculate to what degree the situation just described applies to other complex systems. So far, some indications of generality come from our previous TSP analysis [27] which was the first application of the lid method, and from earlier work of Aarts et al. [56]. These workers did a careful study of the mean energy vs. temperature in a 100 city TSP problem. They found an s-shaped curve with most of the change taking place in a quite narrow temperature range and concluded that the density of state had to be exponential close to the ground state configuration. They also give references to several other investigations, where the same behavior was found. These authors do not explicitly distinguish between the global density of states and the local density of states within a trap. However, as Monte Carlo simulations typically do get trapped at low temperature, we think that this conclusion is similar to ours. Finally, exhaustive enumeration of the configurations of 'on lattice' glass models [57] points in the same direction.

We do not have a detailed theoretical understanding of the origin of the exponential growth of available volume with the barrier and of the exponential character of the local density of states. Qualitatively the phenomenon seems related to the paucity of effective connections in regions of state spaces where the overwhelming majority of the states are energetically unavailable. In this situation, which is not limited to spin glasses, the gradual uncovering of new states as the barrier increases is similar to a branching process, with the barrier in lieu of the time. If the sets of 'children' of two different states are disjoint, exponential growth of the pockets volume follows. The fact that most states are energetically close to their parent is a matter of continuity, which together with the exponential growing volume then gives an exponential local density of states.

Acknowledgments: I am indebted to Richard Frost of the San Diego Supercomputing Center for good advice on the principles of parallel computing and to Ruud Van der Pas of the European High Performance Computing Team, SGI, for his feed-back during the development phases of the code, for his prolonged assistance in performance tuning and for actually running the most memory intensive calculations on hardware which was kindly put at the projects disposal by Silicon Graphics Advanced Technology Center in Cortaillod, Switzerland. It is a pleasure to thank Peter Salamon and the department of Mathematical Sciences at San Diego State University for their nice hospitality during my sabbatical leave of absence and Richard Palmer for comments on this work. I would also like to thank the Santa Fe Institute of Complex Studies where part of this work was done, and the Danish National Research Council (Statens Naturvidenskabelige Forskningsråd) for generous financial support.

[1] K. H. Fischer and J. A. Hertz. *Spin glasses*. Cambridge Univ. Press, 1991. Chapt. 9 of this book reviews the dynamical behavior of spin-glasses, and Chapt. 14 makes the connection to more general issues of the physics of complexity.

[2] E. Vincent, J. Hamman and M. Ocio in : *Recent Progress in Random Magnets*, D. H. Ryan ed., Mc Gill University, Montreal, 1992.

[3] J.-O. Andersson, J. Mattsson and P. Svedlindh. *Phys. Rev. B*, 46:8297, 1992; 48:1063, 1994.

[4] J.-O. Andersson, J. Mattsson and P. Nordblad. *Phys. Rev. B*, 48:13977, 1992.

[5] J.-O. Andersson, J. Mattsson and P. Svedlindh. *Phys. Rev. B*, 48:1063, 1994.

[6] H. Rieger. *J. Phys. A: Math. Gen.* 26:L615, 1993.

[7] L. Lundgren, P. Nordblad, P. Svedlindh, and O. Beckman. *J. Appl. Phys.*, 57:3371, 1985.

[8] M. Alba, M. Ocio, and J. Hammann. *Europhys. Lett.*, 2:45, 1986.

[9] L. Sandlund, P. Svedlindh, P. Granberg, P. Nordblad and L. Lundgren. *J. Appl. Phys.*, 64:5616, 1988.

[10] J. Mattsson, P. Granberg, P. Nordblad, L. Lundgren, R. Loloee, R. Stubi, J. Bass and J. A. Cowen. *J. Magn. Magn. Mat.*, 104-107:1623, 1992.

[11] J. Mattsson, J.-O. Andersson and P. Svedlindh *J. Magn. Magn. Mat.* 194-196:305, 1994.

[12] M. Lederman, R. Orbach, J. Hammann, M. Ocio, and E. Vincent. *Phys. Rev. B* , 44:7403, 1991.

[13] F. Lefloch, J. Hammann, M. Ocio and E. Vincent. *Europhys. Lett.*, 18:647, 1992.

[14] A. J. Bray and M. A. Moore. *Phys. Rev. Lett.*, 58:57, 1987.

[15] D. S. Fisher and D. A. Huse. *Phys. Rev. B* 38:373, 1988.

[16] G. J. M. Koper and H. J. Hilhorst. *J. Phys. (Paris)*,49:429, 1988.

[17] G. Parisi. *Phys. Rev. Lett.*, 50:46, 1983.

[18] C. M. Newman and D. L. Stein *Phys. Rev. Lett.*, 76:515, 1996.

[19] G. Parisi. *cond-mat preprint 9603101* at <http://www.sissa.it>

[20] D.L. Stein and C. M. Newman. *Phys. Rev. E* 51:5228, 1995.

[21] Jorge Korchan and Laurent Laloux. *J. Phys. A: Math. Gen.* 29:1929, 1996.

[22] C. Uhlig, K. H. Hoffmann and P. Sibani. *Zeit. Phys. B* 96:409, 1995.

[23] P. Sibani and K. H. Hoffmann. *Physica A*, 234:751, 1997.

[24] Chandan Dasgupta, Shang-keng Ma and Chin-Kun Hu. *Phys. Rev. B*, 20:3837, 1979.

[25] P. Sibani and J.-O. Andersson *Physica A*, 206:1, 1994.

[26] J.-O. Andersson and P. Sibani. *Physica A*, 229:259, 1996.

[27] P. Sibani, C. Schön, P. Salamon and J.-O. Andersson *Europhys. Lett.* 22:479, 1993.

[28] P. Sibani and P. Schriver *Phys. Rev B* 49:6667, 1994.

[29] U. Krey. *J. Magn. Magn. Mater.* 6:27, 1977

[30] R. Palmer. *Adv. Phys.*, 31:669, 1982.

[31] K. H. Hoffmann, S. Schubert and P. Sibani. to appear in *in Europhys. Lett.*

[32] W. L. McMillan *Phys. Rev. B* 30:476, 1984; *Phys. Rev. B* 29:4026, 1984.

[33] A. J. Bray and M. A. Moore *Phys. Rev. B* 31:631, 1985.

[34] R. N. Bhatt and A. P. Young *Phys. Rev. Lett.* 54:924, 1985.

[35] A. T. Ogielski and I. Morgenstern *Phys. Rev. Lett.* 54:928, 1985.

[36] P. Sibani and R. Van der Pas. *In preparation*.

[37] S. F. Edwards and P. W. Anderson *J. Phys. F* 5:89, 1975.

[38] R. N. Bhatt and A. P. Young *Phys. Rev. B* 37:5606, 1988.

[39] H. Rieger, L. Senten, U. Blasum, M. Diehl, M. Jünger and G. Rinaldi *J. Phys. A: Math. Gen.* 29:3939, 1996

[40] L. Bernardi and I. A. Campbell *Europhys. Lett.*, 26:147, 1994.

[41] D. A. Huse. *Phys. Rev. B* , 43:8673, 1991

[42] S. Grossmann, F. Wegner and K. H. Hoffmann *J. Phys. Lett. (France)* , 46:575, 1985;

[43] K. H. Hoffmann, S. Grossmann, and F. Wegner. *Z. Phys. B*, 60:401, 1985.

[44] R.G. Palmer, D. L. Stein, E. Abrahams, P.W. Anderson *Phys. Rev. Lett.* 53:958, 1984.

[45] I. A. Campbell. *Phys. Rev. B*, 33:3587, 1986.

[46] P. Sibani. *Phys. Rev. B* , 35:8572, 1987.

[47] K. H. Hoffmann and P. Sibani. *Phys. Rev. A*, 38:4261, 1988.

[48] P. Sibani and K. H. Hoffmann. *Phys. Rev. Lett.*, 63:2853, 1989.

[49] K. H. Hoffmann and P. Sibani. *Z. Phys. B*, 80:429, 1990.

[50] C. Schultze, K. H. Hoffmann, and P. Sibani. *Europhys. Lett.* , 15:361, 1991.

[51] K.H. Hoffmann, T. Meintrup, P. Sibani and C. Uhlig. *Europhys. Lett.*, 22:565, 1993.

[52] A. T. Ogielski and D. L. Stein. *Phys. Rev. Lett.*, 55:1634, 1985;

- [53] M. Schreckenberg. *Z. Phys. B*, 60:483–488, 1985
- [54] P. Sibani. *Phys. Rev. B*, 34:3555, 1986.
- [55] P. Sibani and K. H. Hoffmann. *Europhys. Lett.*, 16:423, 1991.
- [56] E. H. L. Aarts, J. H. M. Korst and P. J. M. van Laarhoven. *J. Stat. Phys.*, 50:189, 1988
- [57] J. Christian Schön. *Personal communication*. See also *J. Phys. A: Math. Gen.* 30:2367, 1997, for an analysis of how simulated annealing can find good solutions in complex landscapes with multiple minima each with an exponential local density of states. Given the widespread success of simulated annealing in complex glassy system, this further motivates studying more examples.

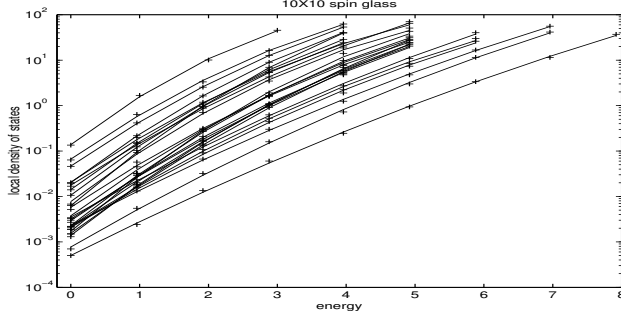


FIG. 1. The local density of states in a state space pocket surrounding a deep energy minimum is shown as a function of the energy in a semilogarithmic plot, for 25 different realizations of the couplings in a 10×10 system. The data points are marked by plusses while the full lines are fits of $\log \mathcal{D}$ to a parabola. Each curve ends at an energy close to the reversal barrier L_{rev} . As we have for convenience normalized the integral of the density of states to one, the great differences in magnitude among the data sets reflect the corresponding variation in the size of the pockets.

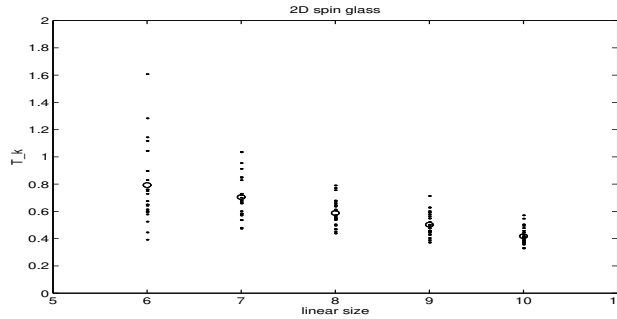


FIG. 2. Each of the displayed dots is the kinetic transition temperature T_k of one realization of a system with a linear size given by the abscissa. T_k is the reciprocal of the coefficient of the linear term in an expansion of the logarithm of the local density of states $\log \mathcal{D}$ to second order in E . The (disorder) average of the distribution is indicated by circles.

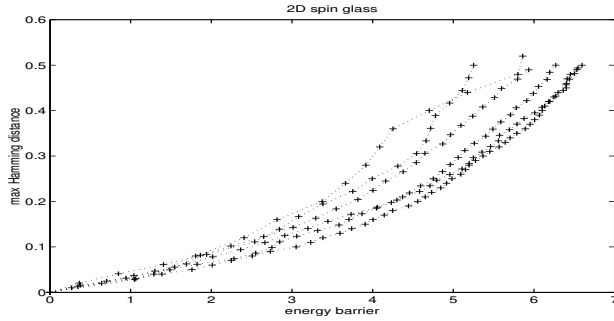


FIG. 3. For each curve, the ordinate is the largest possible fraction of spins which we can be overturned starting from a reference state of very low energy and without overcoming an energy barrier whose value appears as the abscissa. The data are averaged over 25 different disorder realizations. From top to bottom, the curves pertain to systems of size $5^2, 6^2 \dots 10^2$. Data points are shown as pluses while lines are mere guides to the eye. The end point of the curves has ordinate 1/2, indicating that half of the spins in the reference state are overturned at the corresponding barrier values on the abscissa.

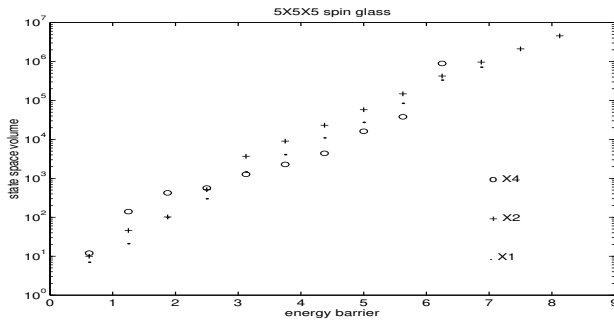


FIG. 4. The plot shows some instances of the exponential dependence of the volume of a pocket on the energy barrier which delimits it. This type of dependence is characteristic of all our data. The data describe the volume vs. barrier relationship in disjoint pockets of the same system. As the exhaustive search is in each case carried out up the reversal barrier, it is possible to find the reverse of the reference state in one pocket without visiting the states belonging any of the others. For convenience, the data have been multiplied by different factors as indicated in the figure itself.

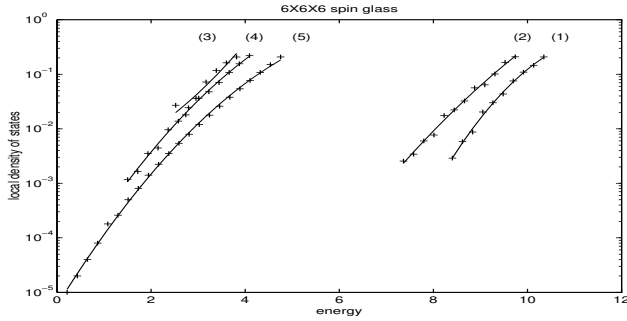


FIG. 5. The data in this plot describe a series of ‘shallow’ pockets rather than deep ones. This is meant to illustrate the valley structure which a system quenched from a high energy state might encounter on its way down to the low energy part of the landscape. All data pertain to a single 6^3 system. The rightmost data set is the local density of states obtained by starting the exhaustive search in a rather poor local energy minimum (energy = $-1.605716J/\text{spin}$) and stopping the search as soon as a lower energy minimum is found. This latter configuration (energy = $-1.610523J/\text{spin}$) is the starting point for a new search, leading to the density of states depicted in the second set of data. In general, we use at each stage the best far configuration as a starting point for the search, which terminates when an even better state is found. The density of states of the pockets generated in this fashion is plotted in the figure. The values of the energy per spin of the reference states – besides the two just mentioned – are -1.632942 , -1.637671 and $-1.643615J/\text{spin}$. Good minima have energies of about $-1.7J/\text{spin}$. For convenience we have used the total energy of the very lowest energy configuration as the origin of the abscissa. We have also normalized the densities by dividing with the total number of states in the pocket.

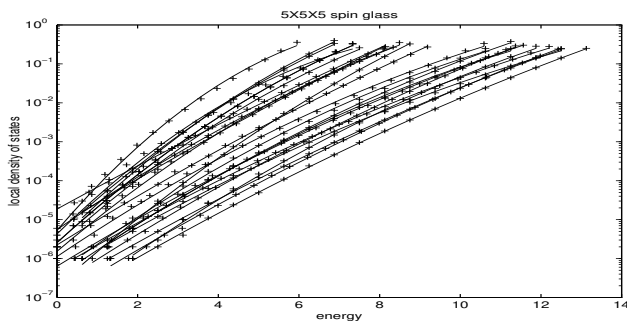


FIG. 6. This figure is the three dimensional counterpart of Fig.1. The local density of states in a state space pocket surrounding a deep energy minimum is shown as a function of the energy in a semilogarithmic plot, for 25 different realizations of the couplings in a $5 \times 5 \times 5$ system. The data points are marked by plusses while in each case the full lines describe fits of $\log \mathcal{D}$ to a parabola. Each curve ends at an energy close to the reversal barrier L_{rev} . As we have for convenience normalized the integral of the density of states to one, the great differences in magnitude among the data sets reflect the corresponding variation in the size of the pockets.

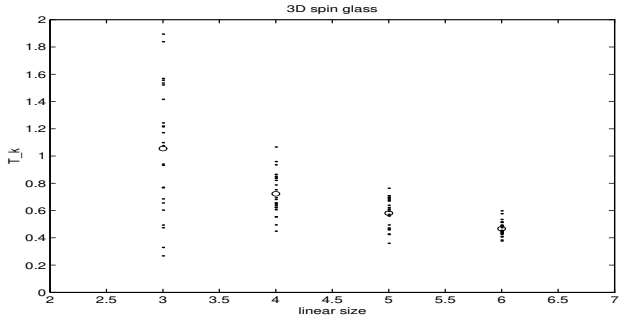


FIG. 7. For several values of the systems' linear size we display as a dot the kinetic transition temperature T_k of 25 different systems of that size. The value of T_k is the reciprocal of the coefficient of the linear term in an expansion of the logarithm of the local density of states $\log \mathcal{D}$ to second order in E . The average value of T_k is indicated by a circle.

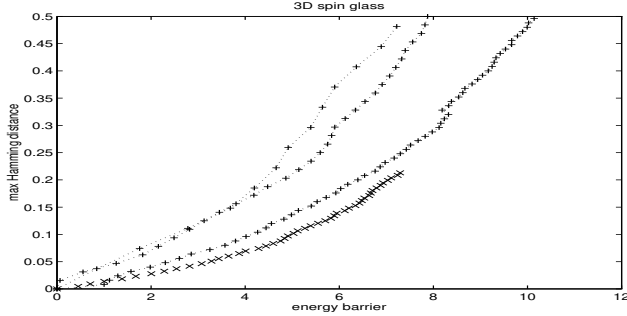


FIG. 8. For each curve, the ordinate is the largest possible fraction of spins which we can be overturned starting from a reference state of very low energy and without overcoming an energy barrier whose value appears as the abscissa. The data are averaged over 25 different disorder realizations. From top to bottom the curves pertain to the 3^3 , 4^3 , 5^3 and 6^3 systems. In the first two cases we were able to reach the (reversal) barrier at which half of the spins can be flipped for all 25 realizations considered. In the 5^3 case we failed in two cases by a few spins. This causes a minor shift in the curve - close to the point 8, 0.3, as there are two missing data sets for higher barrier values. In the case of the 6^3 systems computer memory limits prevented us from reaching the reversal barrier in 15 cases. To avoid the bias which results from averaging over progressively smaller data sets, we only display the last curve up to the largest barrier value for which all the 25 data sets are available.